Stochastic origins of the long-range correlations of ionic current fluctuations in membrane channels

Szymon Mercik* and Karina Weron†
Institute of Physics, Wroclaw University of Technology, 50-370 Wroclaw, Poland
(Received 6 June 2000; revised manuscript received 15 November 2000; published 25 April 2001)

An explicit stochastic representation of a stationary ionic current signal recorded from a single channel of a biological membrane is presented. In the framework of the proposed approach we show how the dichotomous time structure of the signal leads to the non-Markovian character of the channel current. The rescaled range Hurst and detrended fluctuation analyses confirm the theoretical result. To investigate the ionic current fluctuations we introduce the Orey index as a statistical method providing additional information on the properties of stochastic processes. In order to reveal any differences between the experimental and reconstructed signals, we apply also the statistical tests to the model-based simulations of the channel action.

DOI: 10.1103/PhysRevE.63.051910 PACS number(s): 87.17.−d, 05.40.−a

I. INTRODUCTION

The problem of determination of the ion current nature is of importance for many reasons [1–12] and its solution may provide a clue to better understanding of the membrane channel action. However, there are known evident cases where the Markovian nature of the potassium current through single channel was detected [13,14], the assumption that the basic kinetics is purely random can be questioned [15,16]. The suggestions of the non-Markovian character of channel currents [15,16] have led to different ideas of testing the Markov versus non-Markov condition in ion channel recordings [16–19].

In this paper we look for stochastic origins of the non-Markovian property found [17,18] in a data set that was recorded from cell-attached patches of adult locust (*Schistocerca gregaria*) extensor tibiae muscle fibers [17,20]. The potassium current (see Fig. 1) through a high conductance locust potassium channel (i.e., BK channel) was obtained by the patch clamp technique with sampling frequency $f_{ex}=10$ kHz and at a voltage of 60 mV. The muscle preparation was bathed in 180 mM NaCl, 10 mM KCl, 2 mM $CaCl_2$, 10 mM 4-(2-hydroxyethyl)-1-piperazineethanesulphonic acid (HEPES), pH 6.8, and the patch pipettes contained 10 mM NaCl, 180 mM KCl, 2 mM $CaCl_2$, 10 mM HEPES, pH 6.8. The sample presents a time series, consisting of 250 000 points and covering, therefore, 25 s of recording. The error of measurements of ionic current is equal to $\Delta I=1$ pA. The non-Markovian character of the data has been first suggested by Fuliński *et al.* [17]. They have used the Smoluchowski-Chapman-Kolmogorov functional equation as the most basic method of testing Markovianity of finite stochastic chains. The method, being very clear and convenient to apply to real data, does not, however, give information on the detailed characteristics of the non-Markovian process. The main characteristics of the ionic current probability density function (PDF), the closed- and open-state distributions, and the autocorrelation function have been brought to light [18] by using procedures based on the kernel and tail estimators, the bootstrap methodology, and the Zipf plots. The results obtained in [18] have provided clear evidence for the non-Markovian character of the single BK channel kinetics. The present work aims at finding the origins of the non-Markovian nature by proposing theoretical reconstruction of the ionic current fluctuations.

The paper is organized as follows. In Sec. II we introduce the notion of quantiles [21–23] by means of which we confirm the stationarity of the investigated signal. The stationarity of the signal enables us to propose in Sec. III a theoretical reconstruction of the stochastic dichotomous channels action, the signature of which is seen in the bimodal current PDF (see Fig. 2). It is the consequence of the current distribution shape that the original experimental series (see Fig. 1) can be split into two distinct groups of states: the mode of lower values of the current interpreted as the closed state of a channel and the mode of higher values of the current interpreted as the open state. The closed- and open-time distributions corresponding to the two channel states with different con-

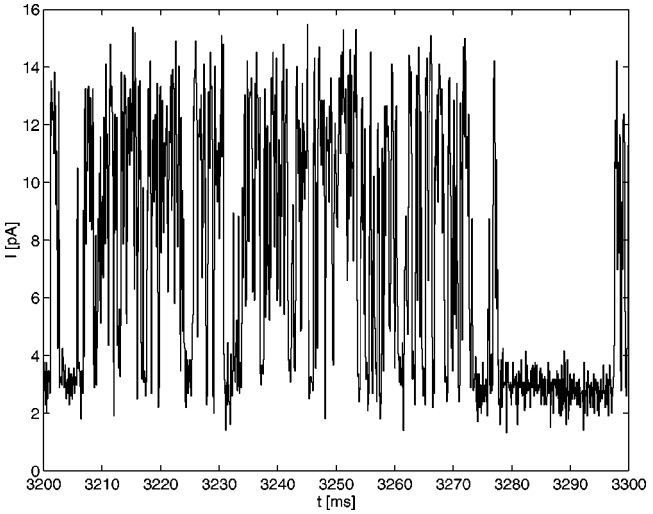

FIG. 1. A part of patch clamp recording of the single BK channel current I (pA) vs time (s), at a pipette potential of +60 mV.

*Email address: mercik@rainbow.if.pwr.wroc.pl
†Email address: karina@rainbow.if.pwr.wroc.pl

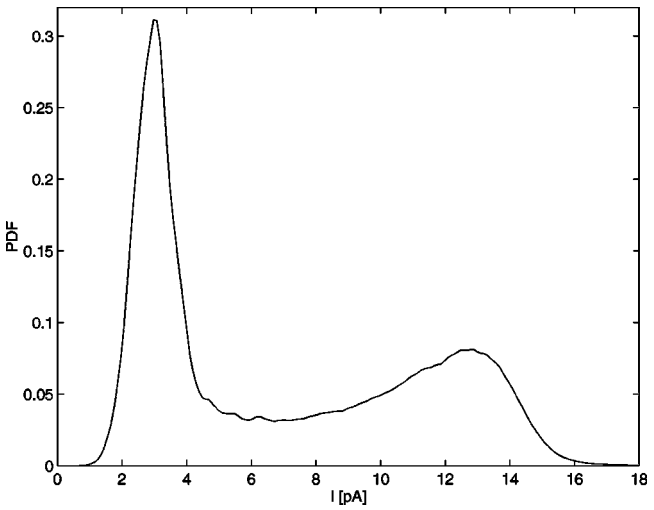

FIG. 2. The experimental ionic current probability density function.

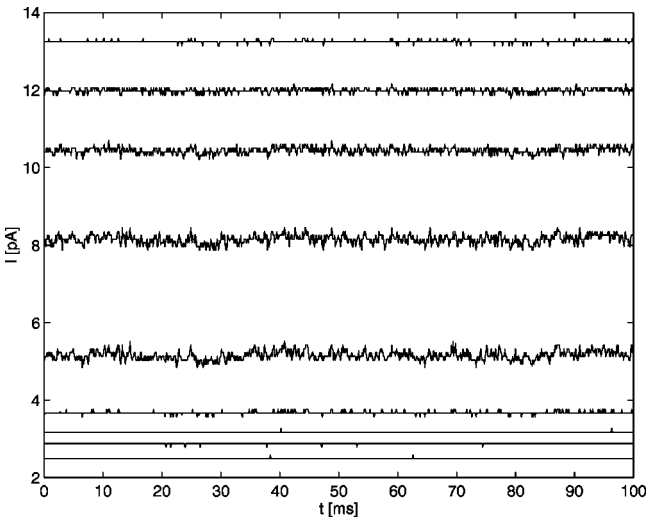

FIG. 3. The quantile lines $k_\varepsilon(t)$ of the original signal of ionic current recorded from a single-membrane channel. The quantiles k_ε are of order from $\varepsilon=0.1$ to 0.9 step 0.1, counting from bottom to top of the figure. The fluctuations are caused by finite lengths of the samples. The estimation errors equal 12% for $\varepsilon=0.5$, 8% for $\varepsilon=0.4$ and 0.6, and 5% for others.

ductances can be obtained if one ''translates'' the record into a dichotomous 0-1 signal, for details see [17,18]. In the framework of the proposed stochastic model of channel action, the long-range correlations (indicating the non-Markovianity of the time series examined) appear as a consequence of the long-tail properties of the closed-time distribution. We check the theoretical result by using different statistical methods of analyzing a stationary time series: the Hurst analysis (in Sec. IV A), the detrended fluctuation analysis (in Sec. IV B), and the Orey index (in Sec. IV C). In an attempt to gain insight as to any differences between the experimental and the reconstructed signals, we apply (in Sec. V) the statistical tests to simulated realizations of the channel action. This procedure helps us to show how much of the experimental signal properties can be explained by a stationary dichotomous stochastic process represented by the theoretical reconstruction of the original time series. Section VI contains the conclusions.

II. STATIONARITY OF THE IONIC CURRENT SIGNAL

Stochastic process X_t is stationary if for all n-element sets of moments $0\leqslant t_1\leqslant t_2\leqslant\cdots\leqslant t_n$, $n=1,2,3,\ldots$, and for all time shifts $\Delta t\geqslant 0$ the n-dimensional distribution of the process fulfills the following condition:

$$P(X_{t_1}>x_1,X_{t_2}>x_2,\ldots,X_{t_n}>x_n)$$
$$=P(X_{t_1+\Delta t}>x_1,X_{t_2+\Delta t}>x_2,\ldots,X_{t_n+\Delta t}>x_n),$$

i.e., the finite-dimensional distributions are independent of time shifts [24,25]. This mathematical definition is rather too complicated to be strictly used in testing the stationarity of a given series and therefore we use simpler and more useful tool—quantiles. A quantile of order $\varepsilon\in[0,1]$ is such a value $k_\varepsilon(t)$ that probability of the recorded signal being less than k_ε at the moment t is equal to ε,

$$P\{X_t\leqslant k_\varepsilon(t)\}=\varepsilon.$$

The quantiles of different orders calculated along the series form a family of lines by means of which one can estimate properties of the investigated process [22,23]. For example, the stationarity property is indicated by quantile lines parallel to the time axis. If the lines are parallel to each other but are not parallel to the time axis, the time series has a constant variance but varies with time mean or, in case when the mean is not well defined, median. If the lines are not parallel to each other, the series does not have a constant variance, or in case of infinite variance, a scale parameter. One can also observe different patterns plotted by the quantile lines: periodicity, pulsations or simply no general rule.

Usually, the quantiles are obtained from a large set of realizations (sample paths) of a particular stochastic process [22,23]. In order to obtain the quantile lines from one sample path only (that is our case) we used the method of ''producing'' a set of paths by cutting [23] the whole record into smaller subrecords (here of length 100 ms). Next, for every moment t we calculated such a real number $k_\varepsilon(t)$ that εth fraction of the subsequences values at the moment t were smaller than $k_\varepsilon(t)$. The quantile lines for the investigated ionic current signal are presented in Fig. 3. The figure shows that, in spite of fluctuations caused by finite lengths of the investigated samples, the lines are time invariant. Notice that there is no periodic behavior or any trend. As a consequence of this observation, we may assume that the studied time series is stationary and has constant mean and variance. The existence and finiteness of the second moment, and hence the mean and variance, result from properties of the current PDF (see Fig. 2), for details see [17,18].

III. DICHOTOMOUS STATIONARY PROCESS WITH LONG-RANGE CORRELATIONS

The ionic current recording (see Fig. 1) reflects the fact that the channels are not permanently open for conduction of

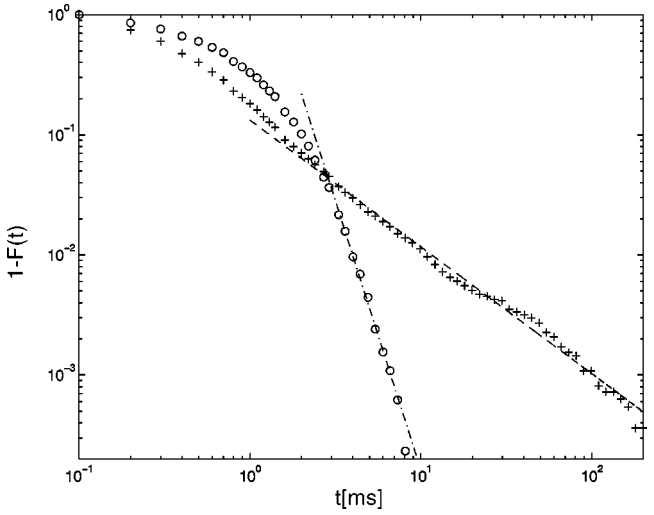

FIG. 4. The tails of the closed- (crosses) and open-time (circles) distributions in log-log scale with fitted lines (dashed line for the closed-time distribution tail and dash-dotted line for open-time distribution tail) suggesting long-time power behavior.

ions but continously switch between closed and open states. The changes are of random nature resulting from, e.g., thermal fluctuations, variations of the voltage difference across the cell membrane, or from conformational changes of channel proteins. The current PDF (see Fig. 2) mirrors two clearly distinct states of the channel: the states of low and high currents corresponding to the closed- and open-channel states, respectively [17,18,20].

In order to model the stochastic dichotomous action let us define two independent sequences of non-negative (nn), independent, identically distributed (iid) random variables: the sequence $\{T_{c,i}\}_{i=0,1,2,\ldots}$, with cumulative distribution function (CDF) $F_c(t)$ and mean $\langle T_c\rangle$, representing periods of closed states and the sequence $\{T_{o,i}\}_{i=1,2,3,\ldots}$, with CDF $F_o(t)$ and mean $\langle T_o\rangle$, representing periods of open states. As it has been already shown [18], the means $\langle T_c\rangle$ and $\langle T_o\rangle$ are finite and take the following values: $\langle T_c\rangle = 0.84 \pm 0.01$ ms and $\langle T_o\rangle = 0.79 \pm 0.01$ ms. On the basis of the studies of the empirical CDF it has been concluded by us [18] that both dwell-time distributions are power tailed (see Fig. 4). In order to test this result we examine here, using a kernel estimator [18,21,22], the PDF's of the closed-and open-state times. The result obtained for the closed-times PDF is presented in Fig. 5. For large t it reveals the power-law behavior

$$f_c(t) = \frac{dF_c(t)}{dt} \propto t^{-(D_c+1)}, \tag{3.1}$$

with $D_c = 1.24 \pm 0.06$, which confirms the previously obtained result [18]

$$P\{T_c > t\} = 1 - F_c(t) \propto t^{-D_c}. \tag{3.2}$$

The studies performed for the open-times PDF give, however, the result different from that obtained in [18]. As it is evident from Fig. 6 the open-times PDF is better fitted by an exponential function

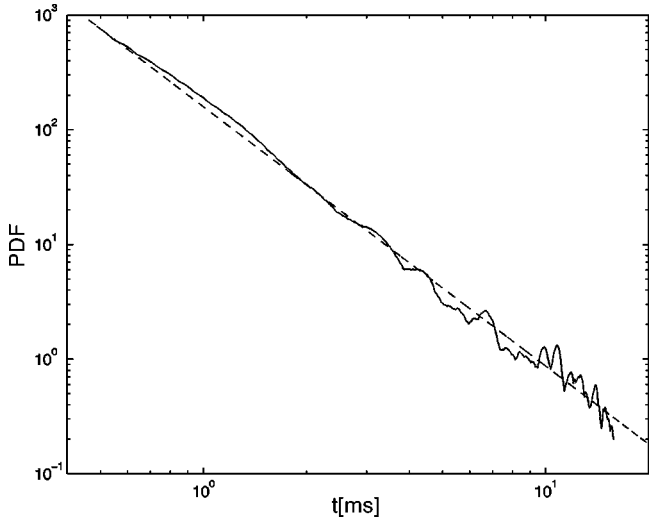

FIG. 5. The PDF of the closed times, Eq. (3.1), plotted in the log-log scale. The slope of the straight line equals -2.24 ± 0.06.

$$f_o(t) = \frac{dF_o(t)}{dt} \propto e^{-\lambda_o t}, \tag{3.3}$$

leading to the exponential tail of the open-times CDF

$$P\{T_o > t\} = 1 - F_o(t) \propto e^{-\lambda_o t}, \tag{3.4}$$

with $\lambda_o = 1.20 \pm 0.08$(1/ms). The expected value of the exponentially distributed open time equals $1/\lambda_o = 0.83 \pm 0.06$ ms and is of order of the mean value $\langle T_o\rangle$ obtained in [18].

Using the above assumptions, one can construct the renewal sequence

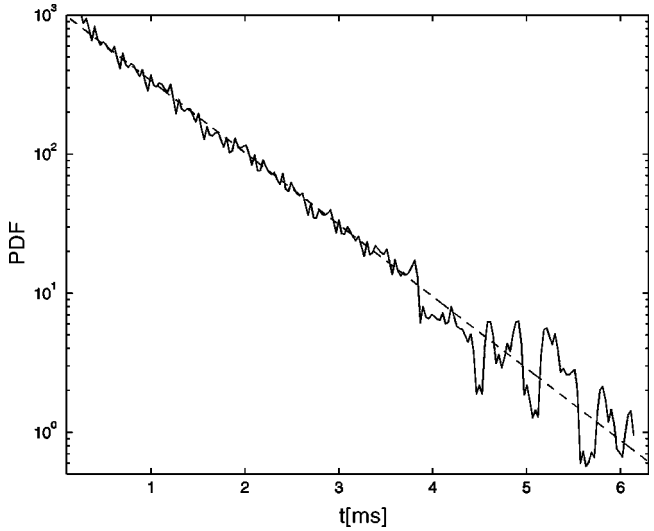

FIG. 6. The PDF of the open times, Eq. (3.3), plotted in the semilogarithm scale. The slope of the straight line equals -1.20 ± 0.08.

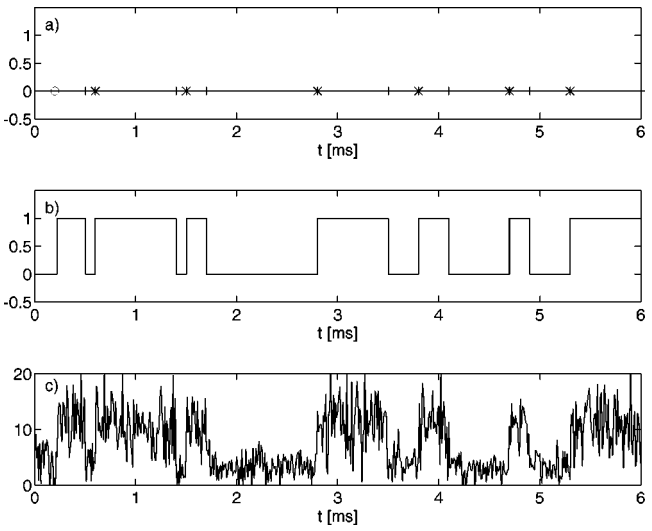

FIG. 7. A sample realization of the three main steps of reconstructing the current signal: (a) a series $\{T_n\}_{n=1,2,3,\ldots}$ (stars) with open times $\{T_{o,i}\}_{i=1,2,3,\ldots}$ (ticks) and τ (circle); (b) a dichotomous signal $L(t)$; (c) a current signal $I(t)$.

$$\{T_k\}_{k=0,1,2,\ldots}=\left\{\tau,\tau+\sum_{i=1}^{k}(T_{c,i}+T_{o,i}),\ \ k=1,2,\ldots\right\} \tag{3.5}$$

that describes instants of time when the channel opens [see Fig. 7(a)]. Random variable τ denotes a delay time, i.e., an interval of time between switching on and the onset of steady measurements. Stabilization of the signal is expressed by the stationarity of the time series. The random delay time can be constructed [26,27] by means of the Bernoulli random variable B [24–29] that is the indicator function of an event of probability p. The probability p that at $t=0$ the channel was open equals

$$p=P\{B=1\}=\frac{\langle T_o\rangle}{\langle T_c\rangle+\langle T_o\rangle},$$

while the probability that at $t=0$ the channel was closed

$$P\{B=0\}=1-p.$$

The delay period consists of closed- and (or) open-states because the channel always has to be in one of these two states. If so, we need to define independent nn random variables $T_c^{(0)}$ and $T_o^{(0)}$ (also independent on $\{T_{c,i}\}_{i=0,1,2,\ldots}$, $\{T_{o,i}\}_{i=1,2,3,\ldots}$, and B) that represent the closed and open times during the delay period. The random variables have distributions defined as

$$P\{T_c^{(0)}<t\}=\frac{1}{\langle T_c\rangle}\int_0^t[1-F_c(s)]ds,$$

$$P\{T_o^{(0)}<t\}=\frac{1}{\langle T_o\rangle}\int_0^t[1-F_o(s)]ds.$$

The renewal sequence $\{T_k\}_{k=0,1,2,\ldots}$ in Eq. (3.5) describes moments when the channel opens and here the delay time τ has to finish with a closed state. As a result of this requirement the delay variable τ decomposes into open- and (or) closed-state periods just like the subsequent interarrival intervals do,

$$\tau=(T_o^{(0)}+T_{c,0})B+T_c^{(0)}(1-B). \tag{3.6}$$

The delay variable (3.6) with distribution (CDF) [27]

$$P\{\tau<t\}=\frac{1}{\langle T_c\rangle+\langle T_o\rangle}\int_0^t\{1-[F_c*F_o](s)\}ds,$$

where $[F_c*F_o](t)$ denotes convolution of two functions $F_c(t)$ and $F_o(t)$, ensures that the renewal series $\{T_k\}_{k=0,1,2,\ldots}$ constructed in Eq. (3.5) is stationary. The stationary sequence of random variables that describes the appearance of the closed and open-states allows us to define stochastic process $L(t)$ that switches the channel on and off [see Fig. 7(b)]

$$L(t)=B\mathbf{1}_{[0,T_{o,0})}(t)+\sum_{n=0}^{\infty}\mathbf{1}_{[T_n,T_n+T_{o,n+1})}(t), \tag{3.7}$$

where

$$\mathbf{1}_{[a,b)}(x)=\begin{cases}1 & \text{if} \quad x\in[a,b)\\ 0 & \text{if} \quad x\notin[a,b)\end{cases}$$

is the indicator function. The process $L(t)$ is stationary with the mean equal to the mean value of the random variable B. On the basis of the dichotomous process $L(t)$ one can construct further a stochastic model of the ionic current fluctuations [see Fig. 7(c)]. Assume that the current is recorded with frequency f_{ex} so that a single record lasts $\Delta t=1/f_{ex}$. Let us define two independent series $\{I_{c,n}\}_{n=1,2,3,\ldots}$ and $\{I_{o,n}\}_{n=1,2,3,\ldots}$ of independent random variables denoting the current that flows through closed and open channel in nth moment of duration Δt. The I_c's have identical distribution with mean $\langle I_c\rangle=m$ and the I_o's are also identical distributed with mean $\langle I_o\rangle=M$. The analysis of the experimental data shows [18] that $m=3.2\pm0.1$ pA and $M=11.0\pm0.1$ pA. The standard deviations of variables from both families are finite and read $\sigma_c=0.82\pm0.05$ pA and $\sigma_o=2.54\pm0.08$ pA for the closed and open state, respectively. Note, that the variances of the estimators used to calculate the standard deviations and means are less then the measurement error ($\Delta I=1$ pA) what reflects the estimators' consistency [21,22,28]; if an estimator is consistent then its volatility tends to zero as the sample length increases. Moreover, the ratios of the standard deviation and the mean value of the ionic current in both states are similar: $\sigma_c/m=0.26\pm0.03$ and $\sigma_o/M=0.23\pm0.02$ that suggests that the higher value of standard deviation σ_o of ionic current in open states is a consequence of the higher current values rather than an intrinsic physical mechanism.

The current recorded in nth moment can be defined as

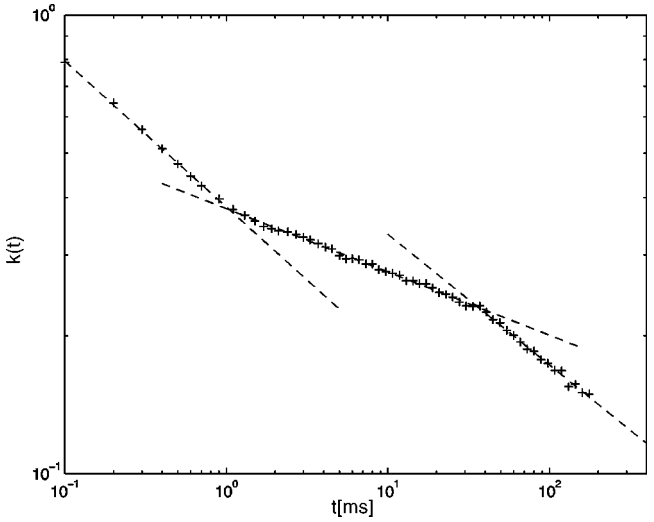

FIG. 8. The autocorrelation function of the experimental current signal decreases with three different power laws: $t^{-\alpha_\kappa}$ where $\alpha_\kappa = 0.32 \pm 0.04$ for $t < 1$ ms, $\alpha_\kappa = 0.14 \pm 0.02$ for 1 ms$< t <$ 40 ms, and $\alpha_\kappa = 0.28 \pm 0.10$ for $t > 40$ ms.

$$I(n) = L(n\Delta t) I_{o,n} + [1 - L(n\Delta t)] I_{c,n}. \tag{3.8}$$

The process $I(t)$ is stationary and for $t = n\Delta t \to \infty$ its autocorrelation function [27] decays with a power law

$$\kappa(t) \propto \frac{\langle T_c \rangle^2 (M-m)^2}{(D_c - 1)(\langle T_c \rangle + \langle T_o \rangle)^3} K(t) t^{-(D_c - 1)} \propto t^{-0.24 \pm 0.06}, \tag{3.9}$$

determined by the power-tail exponent D_c of the closed-time distribution [see Eq. (3.2)], that is the consequence of the fact that

$$P\{T_c > t\} \gg P\{T_o > t\}, \tag{3.10}$$

i.e., the tail of the open-time distribution is dominated by the tail of the closed-time one. $K(t)$ in formula (3.9) denotes a slowly varying in infinity function, i.e., for every $x > 0$ it holds $K(tx)/K(t) \to 1$ when $t \to \infty$. The autocorrelation function calculated directly from the data using the formula

$$\kappa(t) = \frac{\langle I_s \cdot I_{s+t} \rangle - \mu^2}{\sigma^2}, \tag{3.11}$$

where μ is the mean value of the sample and σ^2 is the sample's variation, is presented in Fig. 8. In the long-time range (for $t > 40$ ms) the autocorrelation function decreases as $\kappa(t) \propto t^{-0.28 \pm 0.10}$. This approach does not recover the three regions observed in Fig. 8. The reasons will be discussed in Sec. V.

The above stochastic construction of the channel action shows that the long-range autocorrelation (3.9) between measurements of the ionic current is directly related to the time series' structure. The long-time non-Markovian property of the current signal indicated by the autocorrelation exponent $\alpha_\kappa = D_c - 1$ results from the connection between the power-tail exponent D_c of the closed-time distribution and the power exponent α_κ.

IV. STATISTICAL ANALYSIS OF THE EXPERIMENTAL DATA

In order to test the results obtained above we apply the Hurst, the DFA, and the Orey index methodologies to study the experimental data described in Introduction (see Fig. 1).

Information about the time series structure, correlations, and its fractal properties is provided by the self-similarity index H [13,30]. Stochastic process $X(t)$ is called self-similar with index H if it has the following property:

$$X(at) = a^H X(t). \tag{4.1}$$

The equality in Eq. (4.1) means that the finite-dimensional distributions of the process on the right- and left-hand side of the equation are the same [24]. For example the Brownian motion is self-similar with $H = 1/2$ and the Lévy flight is self-similar with the index equal to $1/\alpha$, where $\alpha \in (0,2)$. The self-similarity index H can be estimated by statistical methods from realization of a stochastic process.

A. Hurst analysis

The rescaled range analysis developed by Hurst [31] may be used to study correlations in the time series measured at different time scales. To perform the Hurst analysis of a series $\{X_k\}_{k=1}^N$ one has to divide the series into d nonoverlaping segments of length n such that $nd = N$. If the time series $\{X_k\}_{k=1}^N$ was recorded with the frequency f_{ex} the window n corresponds to the time duration $\Delta t = n/f_{ex}$. In the next step, for every mth segment of the original record, $m = 1,2,\ldots,d$, one should calculate the mean

$$\langle X \rangle_m = \frac{1}{n} \sum_{j=1}^{n} X_{(m-1)n+j}$$

and the standard deviation

$$S_m(n) = \sqrt{\frac{1}{n-1} \sum_{j=1}^{n} (X_{(m-1)n+j} - \langle X \rangle_m)^2}$$

and then build the cumulative series $\{Y_{j,m}\}_{j=1}^n$

$$Y_{j,m} = \sum_{k=1}^{j} (X_{(m-1)n+j} - \langle X \rangle_m)$$

for which the range R_m is defined as

$$R_m(n) = \max_j \{Y_{j,m}\} - \min_j \{Y_{j,m}\}.$$

For the whole time series the mean value of the rescaled range equals

$$\langle R/S \rangle(\Delta t) \equiv \left\langle \frac{R(\Delta t)}{S(\Delta t)} \right\rangle \equiv \left\langle \frac{R(n)}{S(n)} \right\rangle = \frac{1}{d} \sum_{m=1}^{d} \frac{R_m(n)}{S_m(n)}$$

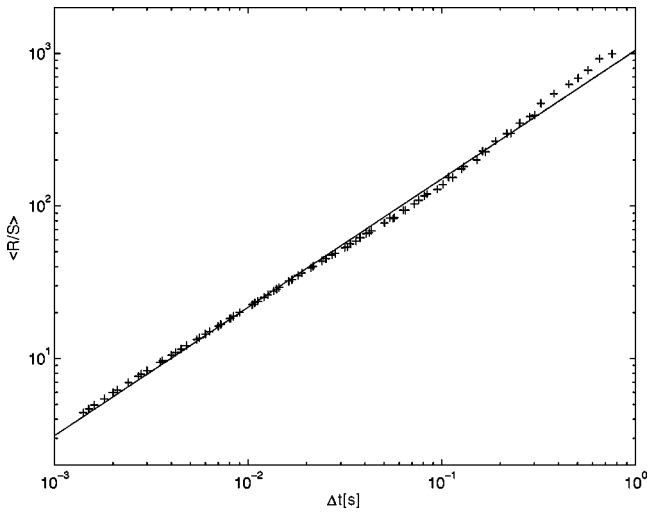

FIG. 9. The rescaled range $\langle R/S\rangle$ as a function of time-lag Δt. The slope of the straight line determines the Hurst exponent in Eq. (12).

and is proportional to Hth power of the duration $\Delta t = n/f_{ex}$

$$\langle R/S\rangle(\Delta t) \propto (\Delta t)^H, \quad 0 < H < 1. \tag{4.2}$$

The value of the Hurst exponent H provides information on the correlations in the time series measured at different time scales. When $H=1/2$, the changes in the values of a time series are random and, therefore, uncorrelated with each other. When $0<H<1/2$, increases in the values of a time series are likely to be followed by decreases and, conversely, decreases are more likely to be followed by increases. Such a time series is called antipersistent. When $1/2<H<1$, increases in the values of a time series are more likely to be followed by increases, and, conversely, decreases are more likely to be followed by decreases. Such a time series is called persistent and it has a long memory property [13].

The Hurst analysis performed for the studied data record is presented in Fig. 9. (To get reliable value of H one should omit the points obtained for $d<10$ because they have too big volatility.) The slope of the Zipf log-log plot of the dependence of the rescaled range mean value $\langle R/S\rangle$ on the duration Δt, Eq. (4.2), determines the Hurst exponent

$$H = 0.84 \pm 0.08.$$

The value of the Hurst exponent indicates that the ionic current signal has the long memory property.

The Hurst exponent H can also be used to estimate the fractal dimension d of the series $X(t)$ taken as a geometrical object [13] embedded in the space $(X(t),t)$,

$$d = 2 - H. \tag{4.3}$$

The fractal dimension of the investigated time series, estimated from the Hurst exponent, equals

$$d = 1.16 \pm 0.08,$$

which is very close to the dimension $d=1.27\pm0.05$ obtained in [18].

With the use of the fractal dimension we can find a formula connecting the Hurst H and autocorrelation α_κ exponents. If the autocorrelation function decays with a power law then the fractal dimension d is related to the power-law exponent α_κ as follows [13]

$$d = 1 + \frac{\alpha_\kappa}{2}. \tag{4.4}$$

It results from Eqs. (4.3) and (4.4) that the Hurst exponent H and the power-law exponent α_κ fulfil the relation

$$H = 1 - \frac{\alpha_\kappa}{2}.$$

B. Detrended fluctuation analysis

An alternative method of testing scaling and correlation properties of a time series is the detrended fluctuation analysis (DFA) [32–34]. The DFA method consists of two steps: the first step is to divide the entire series of length N into N/l nonoverlapping fragments of l observations and determine a local trend of the subseries. Next, one has to define the detrended process in an every fragment denoted by $y_l(n)$ as the difference between the original value of the series and the local trend. The desired statistic is the mean variance of the detrended process $F_d^2(l)$, where mean is taken over all the fragments of size l

$$F_d^2(\Delta t) = \frac{1}{N} \sum_{l=1}^{N/l} \sum_{n=1}^{l} y_l^2(n),$$

where $\Delta t = l/f_{ex}$. Similarily as in the case of the Hurst exponent discussed in Sec. IV A, if only short-range correlations (or no correlations at all) exist in the studied series then $F_d(\Delta t) \propto (\Delta t)^{1/2}$; if there is a long-range power-law correlation then $F_d(\Delta t) \propto (\Delta t)^\alpha$ with $\alpha \neq 0.5$. Moreover, if the exponent α is greater than 0.5, the time series is persistent and if $\alpha<0.5$ then the time series is not persistent.

The result of the DFA analysis of the ionic current is presented in Fig. 10. The slope of the straight line equals $\alpha = 0.89 \pm 0.07$.

C. Orey index

The Orey index γ is a method of the time series data analysis. It was recently proposed [35] for analysing financial data sets. The Orey index estimates the self-similarity index H of stationary Gaussian stochastic processes. It provides an additional information about properties of a time series, completing the Hurst and DFA analyses. Namely, the equivalence of the Orey index and the self-similarity index H (obtained by other statistical methods) suggests the Gaussian nature of the investigated process. The advantage of the Orey index is that it is obtained with one compact formula and one

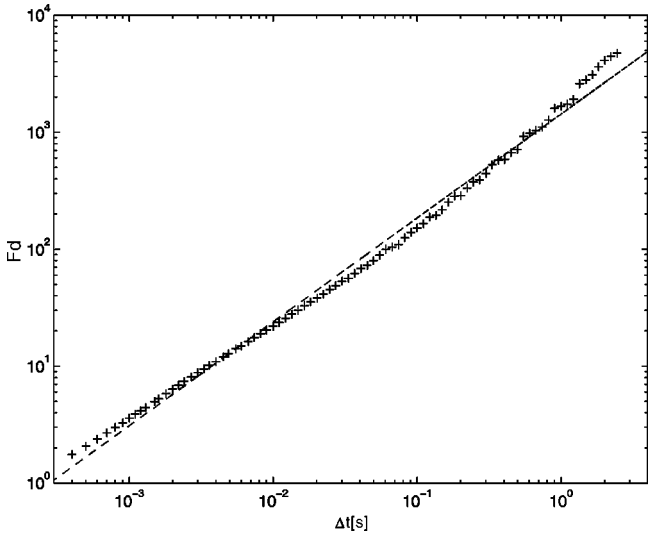

FIG. 10. The dependence of F_d on the time-lag Δt in the detrended fluctuation analysis. Plot in log-log scale determines the power exponent α.

does not need additional tools (like linear regression and the log-log plot) to estimate the self-similarity index of a Gaussian process.

The Orey index γ can be estimated [35,36] by means of an ordinary least squares estimator $\hat{\gamma}^{OLS}$. For a given time series $\{\Delta X_i; i=1,2,\ldots,2^m\}$ consisting of 2^m observations we have to calculate a cumulative series $\{X_j=\Sigma_{i=1}^{j}\Delta X_i; j=1,2,\ldots,2^m\}$ and an incremental variance

$$u^2(n)=\frac{1}{2^n}\sum_{j=1}^{2^n}(X_j-X_{j-1})^2,$$

where $X_0=0$ and $n=1,2,\ldots,m$. Then the Orey index estimator is given by

$$\hat{\gamma}^{OLS}=\sum_{j=1}^{m} y_j \log_2 u(j),$$

where $y_j=(x_j-\overline{x})/\Sigma_{j=1}^{m}(x_j-\overline{x})^2$ and $x_j=\log_2 1/2^j=-j$ for $j=1,2,\ldots,m$. This estimator is strongly consistent with the Orey index γ (for details see [35]).

The calculations of the Orey index were performed with $m=17$, using hence the time series of length equal to 131 072. Because the total length of the time series was equal to 250 000, the calculations were repeated by setting subseries of constant lengths 131 072 in different starting points. It has been found that the Orey index equals

$$\gamma=0.84\pm0.04$$

and does not depend on shifts in time, which also confirms the stationarity of the investigated signal (see Sec. II). The agreement of the Orey index with the self-similarity index H indicates that the transport of ions through a single-membrane channel is Gaussian, i.e., the ionic current process' finite-dimensional distributions are Gaussian. Because

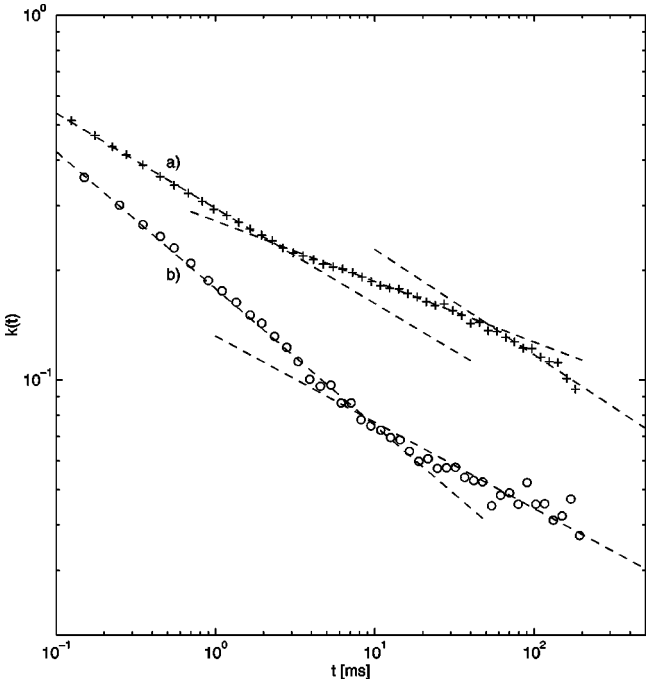

FIG. 11. The autocorrelation functions of two simulated current signals decrease: (*a*) with three different power laws $t^{-\alpha_\kappa}$ with $\alpha_\kappa=0.26\pm0.07$ for $t<3$ ms, $\alpha_\kappa=0.17\pm0.05$ for 3 ms$<t<$40 ms, and $\alpha_\kappa=0.29\pm0.10$ for $t>40$ ms; (*b*) with two different power-laws $t^{-\alpha_\kappa}$: $\alpha_\kappa=0.38\pm0.06$ for $t<8$ ms and $\alpha_\kappa=0.24\pm0.09$ for $t>8$ ms.

the self similarity index $H\neq1/2$, we claim that the process can be identified with a fractional Brownian motion (fBm). The fBm is the only Gaussian self-similar process with the self-similarity index $H\neq1/2$ [37,38].

V. COMPUTER SIMULATIONS OF THE RECONSTRUCTED IONIC CURRENT SIGNAL

In order to get information on differences between the experimental and reconstructed signals, in this section we apply the statistical tests to the model-based simulations of the channel action. Our aim is to show how much of the experimental signal properties can be explained by theoretical reconstruction of the original ionic current time series. The most interesting point is to find conditions under which the reconstructed signal autocorrelation function has properties similar to those observed in the experimental series. The technique of limit theorems of probability theory used to derive this function restricts the theoretical result to the long-time range only. The reason follows from the fact that limit theorems work perfectly on large time scales or large number of random variables only. It is hence clear that we are not able to obtain theoretically the three time-regions (Fig. 8) of the experimental series autocorrelation function. They are seen, however, in some cases of the simulated signal (see Fig. 11).

To perform simulations of the reconstructed ionic current signal (3.8) we need to know the current distributions in the closed- and open-states and the corresponding dwell-time

distributions. Following the results of the first part of Sec. III, we may assume the following.

(A) The current values are distributed according to the Gauss laws with means and standard deviations $m=3.2$ pA and $\sigma_c=0.82$ pA for the closed states and $M=11$ pA and $\sigma_o=2.54$ pA for the open states, respectively.

(B) The open times are distributed according to the exponential law

$$F_o(t)=1-e^{-\lambda_o t},$$

with mean value $\langle T_o\rangle=1/\lambda_o$, where $\lambda_o=1.2(1/\text{ms})$.

(C) The closed times are distributed according to the power-tailed Pareto law

$$F_c(t)=1-\left(a+\frac{t}{\sigma}\right)^{-D_c},$$

where $D_c=1.24$. For simplicity we take $a=1$. The distribution fulfills the condition (3.2). The scale parameter $\sigma=0.201$ ms is determined by the mean value of closed times $\langle T_c\rangle=\sigma/(D_c-1)$.

Taking into account the above assumptions, we generated 500 samples of length 250 000 and calculated the autocorrelation function for each realization of the signal. Two characteristic examples are presented in Fig. 11. It is seen that both autocorrelation functions decrease for large t with the theoretically derived power-law (3.9)

$$\kappa(t)\propto t^{-\alpha_\kappa},$$

where $\alpha_\kappa=0.29\pm0.10$ for the curve indicated by crosses and $\alpha_\kappa=0.24\pm0.09$ for the curve indicated by circles. All of the observed values of α_κ belonged to the interval (0.22,0.31). The wide range of observed values of α_κ's (and other parameters presented below) are caused by highly fluctuating values of generated periods of closed times (note, the power-tailed Pareto distribution with $D_c=1.24$ has no finite variance [21]).

We have found that the autocorrelation function was very sensitive for durations of closed times present in the generated sample. If there was at least one closed state with a long duration (i.e., over 1/100 of the whole sample duration) the autocorrelation function [see curve (*a*) in Fig. 11] ''braked'' the same way as it was observed for the experimental biological data in Fig. 8. If the longest closed state was over 1/10 of the sample duration the autocorrelation function [see curve (b) in Fig. 11] looked different. The maximal value of the closed-time duration in the investigated experimental recording equals 300.8ms and it is about 1/83 of the whole series duration. It was suggested by us [18] that the three different power-law intervals, observed in the experimental signal, are connected with the time structure of the investigated time series. The first scaling region of the autocorrelation function, which is of the same order of magnitude as the average opening and closing times, describes the autocorrelation falloff while the system stays in one state: open or closed. The second scaling region describes the autocorrelation between subsequent, different states of channel (the time range is here larger than the sum of the average opening and closing times, and also than the longest open time duration). The third region of the autocorrelation scaling shows the fastest correlation falloff related to many interstate transitions. The simulations show the conditions under which the two or three different power-law regions may be observed in the reconstructed signal autocorrelation function.

Applying the statistical tests (presented in Sec. IV) to the simulated signal, we have obtained the following values of the Hurst exponent H, the DFA exponent α, and the Orey index γ:

$$H\in(0.66,0.92),\quad \langle H\rangle=0.84\pm0.07,$$

$$\alpha\in(0.69,0.91),\quad \langle\alpha\rangle=0.86\pm0.05,$$

$$\gamma\in(0.70,0.89),\quad \langle\gamma\rangle=0.82\pm0.07,$$

where $\langle\cdot\rangle$ denotes the average value of the corresponding exponent. The above results show the agreement of the main statistical characteristics of both, experimental and reconstructed signals. In our investigations of the reconstructed signal properties we applied different variances of the current in closed and open states. We have found that the convergence is better if the variances are smaller. If the variances are very large (some times larger than the difference of the mean values of current in both states $\sigma_c\approx\sigma_o>M-m$) then the power-law autocorrelation function tail vanished. This is obvious if one realizes that in the case of two states that are not distinguishable, the process became similar to the white noise without any memory. The simulations of different series lengths show that the increase of the generated sample length did not changed significantly the estimated parameters. Also, we did not observe in our studies any significant influence of different current and closed-time distributions, satisfying the conditions taken into account in (A) and (C), respectively.

It is still open question as to what is the role of statistical dependence between closed and open times or the current values. It is well known that the times should be independent [14,39], but on the other hand there are some evidences that the independence may be disturbed [40,41]. Above studies show that the observed long-time correlation, and even the shape of the reconstructed signal autocorrelation function are similar to that observed in the case of experimental data. The result has been obtained without introducing any dependence between the random variables.

VI. CONCLUSIONS

The main objective of the paper was to get information on the stochastic origins of the non-Markovian nature [17,18] of potassium current through a locust potassium channel [17,20]. The detailed knowledge about the channel action (continously switching between closed and open states) is of importance for identification of physical phenomena responsible for the observed ionic current properties. (An influence of internal adsorption [42], ''a crowding'' of ions inside narrow pores [43,44], and of conformational changes of polymer chains [45] has already been pointed out). Taking into account the fact that the recorded current represents a re-

sponse of the whole system, consisting of ions and the channel, the non-Markovian character of the ionic current can be considered as a result of interactions between channel structure and ions inside the channel. The complex state of the whole system, resulting from random interaction of its elements, is clearly reflected in the statistical properties of the current signal.

In contrast to paper [18], where we have given ''prescriptions'' for deriving the statistical characteristics of the experimental data, in present paper we have proposed a theoretical construction of a dichotomous stationary stochastic process with long-range correlations representing the channels action. The applied procedure, based on information obtained in [18], can be summarized in few steps.

(i) Investigation of the stationarity of the ionic current record; here we have used the quantile lines as an easy, practical method of determining the independence of statistical properties of a times series on shifts in time (Sec. II).

(ii) ''Translation'' of the original times series record into a dichotomous 0-1 signal and determination from it the tail properties of the empirical dwell-time distributions. To check the results obtained in [18] for the cumulative distribution functions, here (Sec. III) we have analyzed the properties of the corresponding probability density functions.

(iii) Construction of a stationary process modeling the channel action with an explicit formula of its autocorrelation function, valid in the long-time range (Sec. III).

The theoretically derived autocorrelation function, Eq. (3.9), decreases with a power-law: $\kappa(t) \propto t^{-\alpha_\kappa}$. The power exponent $\alpha_\kappa = D_c - 1$, where $D_c = 1.24 \pm 0.06$ denotes the power-tail exponent of the closed-time distribution, is determined by statistical properties of the channel states with lower values of the ionic current interpreted as the closed states. The value $\alpha_\kappa = 0.24 \pm 0.06 \in (0,1)$ indicates the long memory property of the complex ions channel system and has been confirmed by the results obtained in different statistical studies of the original ionic current record. The values of the autocorrelation exponent α_κ obtained from the definition [Eq. (3.11)] of $\kappa(t)$, from the Hurst analysis, the DFA analysis, and the Orey index are equal, respectively.

$$\alpha_\kappa = 0.28 \pm 0.10,$$

$$\alpha_\kappa = 2(1-H) = 0.32 \pm 0.16,$$

$$\alpha_\kappa = 2(1-\alpha) = 0.22 \pm 0.14,$$

$$\alpha_\kappa = 2(1-\gamma) = 0.32 \pm 0.08.$$

We would like to stress the role of the Orey index [35,36] introduced by us to the analysis of physical signals. The Orey index is a statistical tool identifying the features of stochastic processes directly from their realizations (i.e., from the time series). It carries not only the information about the self-similarity properties of the process but also about its Gaussian nature.

Applying the statistical tests to the model-based simulations of the channel action, we have shown the following.

(i) The agreement of the main statistical characteristics of the reconstructed signal with the corresponding statistical characteristics of the experimental one.

(ii) The influence of time durations obtained in explicit realizations of the random closed-time on the autocorrelation function properties. Note, that those random variables are distributed according to a long-tailed distribution.

The results in our paper show how much of the experimental signal can be explained by a stationary dichotomous stochastic process as represented by the proposed theoretical reconstruction of the channel action. Unfortunately, the results do not indicate the physical mechanisms that might be responsible for the particular dwell-time distributions yielding the observed properties of the experimental signal. For the difference in initial values of both autocorrelation functions [see Fig. 8 and curve (a) in Fig. 11], as well as in their power exponents for short times might be responsible the statistical dependence between the closed and open times already observed in real data [40,41].

ACKNOWLEDGMENTS

We are grateful to Professor P. N. R. Usherwood and Doctor I. Mellor from the University of Nottingham (UK), and to Doctor Z. Siwy from the Silesian University of Technology (Poland) for providing us with the experimental data of ion current through high conductance locust potassium channel. S.M. acknowledges financial support from The Foundation for Polish Science.

[1] B. Robertson and R.D. Astumian, Biophys. J. **57**, 689 (1990).
[2] V.S. Markin, T.Y. Tsong, R.D. Astumian, and B. Robertson, J. Chem. Phys. **93**, 5062 (1990).
[3] V.S. Markin and T.Y. Tsong, Biophys. J. **59**, 1308 (1991).
[4] B. Robertson and R.D. Astumian, J. Chem. Phys. **94**, 7414 (1991).
[5] A. Fuliński, Phys. Rev. Lett. **79**, 4926 (1997); Chaos **8**, 549 (1998).
[6] J.A. Fay, Phys. Rev. E **56**, 3460 (1997).
[7] E. Di Cera and P.E. Phillipson, J. Chem. Phys. **93**, 6006 (1990).
[8] M. Schienbein and H. Gruler, Phys. Rev. E **56**, 7116 (1997).
[9] F. Moss and X. Pei, Nature (London) **376**, 211 (1995).
[10] S.M. Bezrukov and I. Vodyanoy, Nature (London) **378**, 362 (1995); **385**, 319 (1997); Biophys. J. **73**, 2456 (1997).
[11] J.J. Collins, C.C. Chow, and T.T. Imhoff, Nature (London) **376**, 236 (1995); Phys. Rev. E **52**, R3 321 (1995).
[12] D.J. Christini and J.J. Collins, Phys. Rev. Lett. **75**, 2782 (1995).
[13] J. B. Bassingthwaighte, L. S. Liebovitch, and B. J. West, *Fractal Physiology* (Oxford University Press, Oxford, 1994).
[14] B. Hille, *Ionic Channels of Excitable Membranes* (Sinauer Inc., Sunderland, MA, 1992).
[15] D. Petracchi, C. Ascoli, M. Barbi, S. Chillemi, M. Pellegrini,

and M. Pellegrino, J. Stat. Phys. **70**, 393 (1993).
[16] J. Timmer and S. Klein, Phys. Rev. E **55**, 3306 (1997).
[17] A. Fuliński, Z. Grzywna, I. Mellor, Z. Siwy, and P.N.R. Usherwood, Phys. Rev. E **58**, 919 (1998).
[18] Sz. Mercik, K. Weron, and Z. Siwy, Phys. Rev. E **60**, 7343 (1999).
[19] L.S. Liebovitch, A.T. Todorov, M. Zochowski, D. Scheurle, L. Colgin, M.A. Wood, K.A. Ellenbogen, J.M. Herre, and R.C. Bernstein, Phys. Rev. E **59**, 3312 (1999).
[20] E. Gorczyńska, P.L. Huddie, B.A. Miller, I.R. Mellor, R.L. Ramsey, and P.N.R. Usherwood, Pfluegers Arch. Gesamte Physiol. Menschen Tiere **432**, 597 (1996).
[21] L. Devroye, *A Course on Density Estimation* (Birkhäuser, Boston, 1987).
[22] A. Janicki and A. Weron, *Simulation and Chaotic Behavior of α-Stable Stochastic Processes* (Dekker, New York, 1994).
[23] A. Janicki and A. Weron, Stat. Sci. **9**, 109 (1994).
[24] W. Feller, *An Introduction to Probability Theory and its Applications*, 2nd ed. (Wiley, New York, 1971).
[25] P. Billingsley, *Probability and Measure*, 2nd ed. (Wiley, New York, 1986).
[26] S. Resnick, *Adventures in Stochastic Processes* (Birkhäuser, Boston, 1992).
[27] D. Heath, S. Resnick, and G. Samorodnitsky, Math. Op. Res. **23**, 145 (1998).
[28] J.A. Rice, *Mathematical Statistics and Data Analysis* (Duxbury Press, Berkeley, 1995).
[29] Y. Viniotis, *Probability and Random Processes for Electrical Engineers* (McGraw-Hill, Singapore, 1998).
[30] M.S. Taqqu, in *Encyklopedia of Statistical Sciences*, edited by E. Eberlein and M.S. Taqqu (Wiley, New York, 1986).
[31] H.E. Hurst, Trans. Am. Soc. Civ. Eng. **116**, 770 (1951).
[32] C.-K. Peng S.V. Buldyrev, S. Havlin, M. Simons, H.E. Stanley, and A.L. Goldberger, Phys. Rev. E **49**, 1685 (1994).
[33] S.V. Buldyrev, N.V. Dokholyan, A.L. Goldberger, S. Havlin, C.-K. Peng, H.E. Stanley, and G.M. Viswanathan, Physica A **249**, 430 (1998).
[34] G.M. Viswanathan, S.V. Buldyrev, S. Havlin, and H.E. Stanley, Physica A **249**, 581 (1998).
[35] R. Norvaisa and D. M. Salopek (unpublished).
[36] P. Hall and A. Wood, Biometrika **80**, 246 (1993).
[37] B.B. Mandelbrot and J.W. Van Ness, SIAM Rev. **10**, 422 (1968).
[38] G. Samorodnitsky and M.S. Taqqu, *Stable Non-Gaussian Random Processes* (Chapman & Hall, London, 1994).
[39] E. Neher and B. Sakmann, Nature (London) **260**, 799 (1976).
[40] C.J. Kerry, R.L. Ramsey, M.S.P. Sansom, and P.N.R. Usherwood, Biophys. J. **53**, 39 (1988).
[41] F.G. Ball, C.J. Kerry, R.L. Ramsey, M.S.P. Sansom, and P.N.R. Usherwood, Biophys. J. **54**, 309 (1988).
[42] Z.J. Grzywna, L.S. Liebovitch, and Z. Siwy, J. Membr. Sci. **242**, 235 (1998).
[43] Z.J. Grzywna, Z. Siwy, and C.L. Bashford, J. Membr. Sci. **121**, 261 (1996).
[44] Z.J. Grzywna and Z. Siwy, Int. J. Bifurcation Chaos Appl. Sci. Eng. **5**, 1115 (1997).
[45] M. Karplus and J.A. McCammon, Annu. Rev. Biochem. **53**, 263 (1983).